Microstructure and oxidation behaviour at 1100°C of HfC- containing Cr-rich iron-based cast alloys

Patrice Berthod, Elodie Conrath

Microstructure and oxidation behaviour at 1100°C of HfC-containing Cr-rich iron-based cast alloys

Patrice Berthod* and Elodie Conrath

Institut Jean Lamour (CNRS UMR 7198)
Faculté des Sciences et Technologies, Université de Lorraine,
Boulevard des Aiguillettes, BP 70239, F-54506 Vandoeuvre-lès-Nancy, France
*Corresponding author, email: patrice.berthod@centraliens-lille.org

Post-print of the article Materials Science and Technology (2015) 31(14) 1764-1772.
DOI 10.1179/1743284715Y.0000000003

Abstract.

Three alloys containing 0.25 to 0.50wt.%C, 26 to 28wt.%Cr, and also 4 to 6wt.%Hf were elaborated by foundry. They contain a dendritic matrix and HfC carbides. They were exposed in air at 1100°C during 46 hours. The aged microstructures display coarsened chromium carbides but never significant morphological or fraction evolution of the HfC carbides. The surface characterization of the oxidized states shows that the alloys well behave during the 46 hours of exposure to 1100°C, despite some local starts of fast oxidation. The room temperature hardness was modified in all cases by the microstructure stabilization achieved during the high temperature exposure. A preliminary creep test showed that the reinforcement by HfC may lead to interesting mechanical resistance at 1100°C.

Introduction

There are a lot of applications which require alloys able to be used at elevated temperature on long times in severe conditions (mechanical stresses, contact with aggressive liquids, oxidant gaseous environments) and displaying ductility and impact toughness high enough at all temperatures. Besides aeronautical turbine blades, there are many industrial processes which correspond to the previous triple requirements for the used alloys, notably for temperatures as high as 1100°C. This is for example the case of some tools used in the glass-forming industry. Because of their complex geometry many metallic pieces used at high temperature are fabricated by foundry. This elaboration route allows obtaining {coarsened grains}-

microstructures favourable to good mechanical resistance at high temperature[1]. In the chemical composition of the alloys, aluminium, chromium or silicon are present to bring them high resistance against high temperature oxidation[2]. Among these three elements chromium plays a particular role since it brings good resistance to oxidation by gases and to corrosion by aggressive melts[3]. Unfortunately the presence of high chromium content in a high temperature alloy supposes that this one is simultaneously rather poor in aluminium, in order to be not affected by metallurgical instabilities during elaboration or during service. Consequently the refractory alloys the chemical resistance of which is given by chromium, cannot be reinforced by γ/γ' intermetallic precipitates as the single crystal nickel-based superalloys[4]. Solid solution strengthening and/or reinforcement by precipitation of particles as carbides are compulsory. The most common carbides are unfortunately not stable at high temperature to bring the alloys long lasting reinforcement at temperatures higher than 1000°C. For example, during high temperature service, the chromium carbides − which are used in many cast superalloys − tend to morphologically evolve or to disappear. This is also the case of the script-like shaped tantalum carbides which efficiently strengthen many of the cast cobalt-based superalloys. These ones, precipitated at the end of solidification, form an interpenetrated eutectic compound with matrix in the interdendritic spaces. Long exposure at elevated temperature induces TaC fragmentation, with as result a progressive loss of the high creep-resistance initially given by these TaC carbides.

As observed for a cast cobalt-based alloy in an earlier work[5] other MC carbides offer the same advantages as TaC but without such inconvenience: the HfC carbides which may precipitate at solidification with the same script-like shape and the same repartition. These HfC carbides are seemingly more resistant than the TaC ones, against morphologic evolution during long stages at elevated temperature. This allows their strengthening effect staying longer at a high level.

Mechanical reinforcement at high temperature by HfC carbides was obviously only little envisaged: for example for rare Ni-based[6] and Co-based[7] hard metals or superalloys, for some molybdenum-based or tungsten-based or rhenium-based metallic pieces[8-14]... Furthermore, this type of carbide was evidently never thought for iron-based alloys, although the particularly high melting point of iron (1535°C)[15] and the low cost of this element are very interesting for the metallic base of a refractory alloy. In case of good microstructural stability – notably of the reinforcing carbides – and sufficiently high mechanical properties on long term, iron-based alloys may represent very interesting technical-economic alternative materials by comparison with the nickel-based alloys and cobalt-based alloys which are

usually considered for high temperature applications. Elaborating by foundry selected chromium-rich iron-based alloys, observing the microstructure obtained after solidification, studying how the microstructures and the surface states evolve at the rather high temperature 1100°C as well as testing the creep resistance of such alloys at this same temperature are the goals of this work.

Experimental

Synthesis of the alloys and characterization in the as-cast condition

Three hafnium-containing Fe-based alloys and two Hf-free ones (for comparison) were elaborated by foundry. Small parts of pure elements (Alfa Aesar, purity > 99.9wt.%) were weighed to target the compositions of the final alloys with the following contents (in wt.%): {Cr; C; Hf} = {25; 0.25; 0} (Fe25 alloy), {25; 0.50; 0} (Fe50 alloy), {25; 0.25; 3.7} (Hfe25 alloy), {25; 0.50; 3.7} (Hfe50 alloy) and {25; 0.50; 5.6} (HFE50 alloy). The pure elements were heated and melted together in the water-cooled copper crucible of a High Frequency induction furnace (CELES), in a chamber isolated from air by a closed silica tube containing an inert atmosphere of pure argon (300mbars). Solidification and solid state cooling, both occurred in the same copper crucible, followed the isothermal 3 minutes stage in the liquid state. Five 40g-weighing ingots were thus obtained. After return to room temperature, these ingots were cut for obtaining first metallographic samples for the examination of the as-cast microstructures, and second samples devoted to the 1100°C-exposure tests (parallelepipeds with as dimensions: length ≈9 × width ≈7 × thickness ≈3 mm^3). The samples devoted to metallography examinations were embedded in a cold resin mixture (resin CY230 + hardener HY956, ESCIL) then ground (SiC-enriched papers with grade varying from 120 to 1200) and polished (textile containing 1µm-alumina particles) until obtaining a mirror-like state. The microstructure examination was done by using a Scanning Electron Microscope (SEM) JEOL JSM-6010LA: imaging in Back Scattered Electrons (BSE) mode and chemical analysis by Energy Dispersion Spectrometry (EDS).

Exposures at 1100°C and characterization in the aged condition

The samples destined to the exposures at 1100°C were ground with SiC-papers (final grade: 1200), and their edges and corners smoothed (1200-grit paper too). They were weighed then exposed in a furnace traversed by a continuous flow of synthetic air (dry N_2-20%O_2, 1 atm). The applied thermal cycle was composed of a heating at +20K min^{-1}, an isothermal stage of

46h at 1100°C and a cooling rate at -5K min^{-1}. After high temperature exposure the samples were weighed again and metallographically characterized. First the oxidized surfaces were analysed by X-Ray diffraction using a Philips X'Pert Pro diffractometer (for the identification of the external oxides present on surface). A thin gold layer was then deposited all around the oxidized samples by cathodic evaporation. An electrolytic layer of nickel, thick enough in order to limit the loss of external oxide during cutting, was thereafter deposited. The oxidized then coated samples were cut in two parts, embedded in cold resin mixture and polished as described above for the as-cast metallography samples, to allow cross-sections examinations and characterizations (carried out using the same SEM and its EDS apparatus, and the Adobe Photoshop software).

Hardness characterization

The hardness of the alloys before and after exposure to high temperature were measured and compared. Tests were done using a Testwell Wolpert apparatus equipped with a diamond pyramidal penetrator. Indentations were carried out with a 30kg load, following the Vickers method. Three results were obtained for each {alloy, state} combination, for allowing the calculation of an average value and a standard deviation one (thereafter used as uncertainty).

Flexural creep test

In order to get first information about another important property for such alloys devoted to high temperature, a bending test was realized with one of the studied alloys, HFE50. A parallelepiped was cut in the same ingot, with as global dimensions 1 mm × 2 mm × 15 mm. It was thereafter polished on its two main faces with SiC papers and finished with {1µm hard particles}-enriched textile, in order to avoid any stress concentration problems. To perform the creep flexural test a SETARAM TMA dilatometer was modified to allow performing such mechanical bending tests under moderate stress. The sample was placed on two alumina bottom supports separated by 12mm. The load was progressively applied on the top-middle of the sample, until reaching the value required to induce a constant tensile stress of exactly 5 MPa in the bottom-middle of the sample, for the exact sectional dimensions of this one (measured with a precision electronic calliper). The heating was performed at +20K min^{-1} from room temperature to 1100°C, at which the central upper force was continuously applied during almost 100 hours under pure argon. The downward displacement of the upper support was measured by the same sensor as used for measuring the thermal dilatation of samples

during thermo-dilatometry tests. The resulting deformation was recorded every 70 seconds. The maximal possible deformation is about 1.4 mm (before contact of the bottom-middle part of the deformed sample with the base of the alumina apparatus).

Results

Chemical compositions

EDS measurements were performed on the mounted and polished samples using the SEM. The obtained chemical compositions are displayed in Table 1 (SEM/EDS over full ×1000 areas). By looking to the values of standard deviation one can see that the three measurements taken in consideration were rather scattered, consequence of the dispersed coarse carbide particles. However, globally, in all cases the same chromium contents of about 26-28 wt.% (close to the targeted value) were obtained. The targeted Hf contents were also globally obtained: a medium value at 4 - 4.8wt.%, and a high value of 5.8 wt.%.

As-cast microstructures

The SEM/BSE micrographs given in Fig. 1 illustrate the as-cast microstructures of the alloys containing hafnium. Their matrixes are composed of an iron-chromium solid solution. The matrix is mixed with eutectic hafnium carbides in the interdendritic spaces. These HfC carbides appear as white particles on these micrographs taken with the SEM in BSE mode. Another type of hafnium carbides is also present: these other carbides are compact and polygonal. These compact HfC carbides seem having crystallized before the dendritic development of the matrix, at the early start of solidification. These compact carbides are seemingly pre-eutectic ones. Thanks to their compactness and their size they are easier to analyse by EDS spot analysis than the too fine eutectic ones. The measurement results clearly indicate that they are effectively HfC (e.g. 54.4C-40.6Hf or 52.0C-44.4Hf in at.%, rest Fe and Cr).

The Hfe50 alloy is obviously the one of the three Hf-containing ones which contains the lowest quantity of HfC carbides. Logically it is also the one which is the poorest in hafnium: (4 wt.%Hf instead 5 and 6 wt.% for the two other Hf-containing alloys.

Two of these alloys (Hfe50 and HFE50) also contain chromium carbides while no chromium carbides can be seen in the Hfe25 alloy for which the atomic contents in carbon and hafnium are similar. For this alloy the stronger carbide-former element present in the chemical composition – Hf – involved all the carbon atoms to form its carbides (HfC). With twice the

Hfe25 alloy's carbon content, the crystallization of additional carbides of chromium was possible during the solidification of the Hfe50 alloy. These chromium carbides are the particles which appear darker than matrix in the SEM/BSE micrographs. With 6wt.% Hf (the highest hafnium content among the three alloys) the as-cast HFE50 alloy contains less chromium carbides than the Hfe50 alloy, but these ones are present in rather significant quantities. The two ternary alloys, the Fe25 and Fe50 ones, contain only chromium carbides. The latter are unsurprisingly more present in the second alloy (0.50 wt.% C) than in the first one (0.25 wt.% C).

Aged microstructures

After 46 hours spent at 1100°C the microstructures of the alloys have significantly evolved (Fig. 2). During this high temperature exposure the chromium carbides became much rounder in the alloys where they already existed in the as-cast state (Fe25, Fe50, Hfe50 and HFE50). EDS spot analyses carried out on the coarsest of these carbides confirmed that they are chromium carbides, with their high levels in chromium (more 60wt.%) and in carbon (higher than everywhere in the microstructure). Unfortunately EDS is not accurate enough, notably for light elements such as carbon, and it was not possible to specify the formula of these carbides. Thus their identification was only qualitative. Additionally, some rare chromium carbides have precipitated in the Hfe25 alloy which was initially free of such carbides. The eutectic HfC carbides evolved also a little, with a slight decrease in apparent surface fraction and a limited fragmentation affecting the initial script-like morphology of these carbides. In contrast, the compact HfC carbides remained unchanged.

EDS spot analysis was also carried out in the matrix of each aged alloy and the results are graphically displayed in Fig. 3 for Cr (top) and Hf (bottom), together with the same type of results obtained in the as-cast condition. One can see that the chromium content in the matrix of the alloys has generally decreased during the exposure at 1100°C, consequence of the solid state precipitation and coarsening of the chromium carbides. In contrast, the matrixes' contents in hafnium remained unchanged by comparison with the as-cast state: still negligible.

Quantitative analyse of the carbides' surface fractions

A tool present in the Adobe Photoshop software allows measuring the surface fractions of particles displaying different grey levels. Several SEM/BSE micrographs (three randomly taken for each as-cast or aged sample) were analysed after having been decomposed in white

and black pixels by choosing pertinent levels of grey. The surface fractions of each population of carbide were then assessed with an average value and a standard deviation one in each case. The results are given as graphs in Fig. 4. In the as-cast state it appears that the chromium carbides are effectively more present in the Fe50 alloy (about 6 surf.%) than in the Fe25 (about 4 surf.%) one. The as-cast HFE50 alloy seems presenting almost the same surface fraction of chromium carbides as the Fe50 alloy and twice the value measured for the Hf-poorer Hfe50 alloy. The Hfe25 alloy is totally free of any chromium carbides.
In the as-cast condition again, the surface fraction of HfC carbides does not vary significantly among the three Hf-containing alloys (around 3-4 surf.% for the three alloys).

After 46 hours spent at 1100°C the carbide surface fraction did not significantly evolve in the case of the hafnium ones (Fig. 4 bottom), but much more for the chromium carbides (Fig. 4 top). Indeed, if no real increase is seen for the Fe25 alloy the initial surface fraction of chromium carbide significantly increased for the four other ones (typically 5 surf.% more). Notably, chromium carbides have precipitated in the Hfe50 alloy which did not initially contain carbides of this type.

Hardness

Three Vickers indentations were carried out for the five alloys in their as-cast state and in their aged one, at room temperature. In each case the average value and the standard deviation one (uncertainty) were calculated. The obtained results are graphically presented in Fig. 5. The {46h, 1100°C}-ageing obviously induced either a severe loss in hardness (case of the two Hf-free alloys, 50-70 Vickers points lost), or a slight increase (case of the three Hf-containing alloys).

Surface states

At the end of the high temperature stage and after return to room temperature, the oxidized samples were weighed to value the mass gain by comparing with their initial weights (Table 2). Unfortunately the oxides partially spalled off during the cooling, as notably demonstrated with the negative mass variation obtained for the Hfe25 alloy. However sufficient quantities of oxides remained over the oxidized samples to allow performing X-ray Diffraction prior to the gold and nickel deposition, cutting, embedding and polishing. The results are illustrated by two diffractograms given as examples in Fig. 6 (case of the Hf-free Fe25 alloy) and Fig. 7 (case of the Hf-containing Hfe25 alloy). Globally the ternary alloys were covered by chromia but also by oxides of iron and chromium together, with various Fe/Cr ratios. The scales which

appeared over the Hf-containing alloys were composed of chromia but also of oxides of Fe and Cr together. Some hafnium oxides were additionally detected in their cases.

The observations in cross-section are illustrated by some SEM/BSE micrographs in Fig. 8 for the Hf-free alloys and in Fig. 9 and Fig. 10 for the Hf-containing alloys. They allowed confirming and visualizing the presence of the above mentioned oxides, as is to say Cr_2O_3, Fe_2O_3 and the intermediate oxides involving both Cr and Fe on the Fe25 and Fe50 surfaces on one hand, and the same oxides with additionally HfO_2 on the Hfe25, Hfe50 and HFE50 surfaces on the other hand. Cross-section observations also allow observing the thickness of the external scales around the oxidized samples and to detect possible internal oxidation. These multi-constituted oxides tend to be rather thick over the ternary alloys, notably over the Fe25 alloy in which general oxidation obviously consumed the alloy inward, as shown by the high chromium contents in the subsurface, even close to the alloy/scale interface (higher than 24 wt.%Cr, no Cr diffusion acting toward the oxidation front). Helped by a more developed interdendritic network of chromium carbides facilitating Cr diffusion towards the oxidation front, the Fe50 alloy seemingly longer resisted against catastrophic oxidation as shown by numerous subsurface areas where the Cr content is slightly lowered, as shown by the EDS spot measurements in Fig. 8 (bottom) and by the concentration profiles in Fig. 11 (bottom, left). The Hf-containing alloys well behaved as demonstrated by the continuous rather thin Cr-rich M_2O_3 oxide scales and the subsurface only sligthly impoverished in chromium close to the alloy/scale interface (Fig. 9 for the Hfe25 and Hfe50 alloys, and Fig. 10 top for the HFE50 one). However this good behaviour of the Hf-containing alloys will not be much longer maintained as shown by first local starts of fast oxidation (Fig. 9 top, and Fig. 10 bottom) as well as by EDS profiles demonstrating that outward Cr diffusion cannot compete with the {catastrophic oxidation}-powered regression of the oxide/alloy interface (Cr profiles in Fig. 11 top and bottom right).

Creep resistance at 1100°C

A high temperature 3 points bending test was performed on a parallelepiped sample prepared from the HFE50 ingot. The obtained curve, cut at both sides to remove the heating and cooling parts, is showed in Fig. 12. One can see that, after a first part during which the deformation rate was high but decreases (primary creep stage), the deformation became much slower. When the test was stopped (after near a hundred hours) the secondary creep stage was stabilized with a very low deformation rate (of about 0.05 µm per hour).

Discussion

When chromium is the single carbide-former element present in the iron-based alloys (ternary ones) only chromium carbides precipitate during solidification. But when hafnium is also present the HfC crystallize in priority, and chromium carbides may be present in the as-cast state only when there are more carbon atoms than hafnium atoms in the alloy: the as-cast Hfe50 and HFE50 alloys contain both Cr carbides and Hf carbides while the Hfe25 alloy only contains HfC as carbides. A noticeable particularity of the hafnium carbides is that they seem appearing in two steps: the first ones before the dendritic development (or at the same time) and the following ones at the end of solidification. The first ones are compact and the others are script-like shaped, with probably a better efficiency of the later ones for the creep resistance of the alloys.

After a 46h-long stage at 1100°C the surface fractions of the HfC carbides are almost the same while supplementary chromium carbides have precipitated; many of these chromium carbides are then particularly coarse. Despite the fast solidification due to the rapid cooling of the alloys in contact with the water-cooled copper crucible of the induction furnace, the very strong carbide-former element hafnium succeeded in involving the necessary quantity of carbon to form the HfC carbides with all the Hf atoms present in the alloys (as shown by the total absence of Hf in the matrix). At the same time a part of the rest of carbon had given first chromium carbides, but the last carbon atoms have been trapped in the matrix, with as result an overconcentration in carbon of the ferritic phase. This led to alloys which are not in thermodynamic equilibrium. The ferritic matrix oversaturated in carbon evolved during the subsequent stage at 1100°C and the released carbon atoms were combined with chromium since no free hafnium atom was available. This led to the growth of the chromium carbides until obtaining the coarsened chromium carbides visible after return at room temperature. The high solidification rate also led to a too high carbon concentration in the ferritic matrix of the two ternary alloys. During the 1100°C-stage the carbon in excess was released in these ternary alloys too, leading also to a coarsening of the present chromium carbides. The oversaturation in carbon of the ferritic matrix of the as-cast alloys led to a room temperature hardness rather high for a ferritic iron-based structure, especially in the case of the two Hf-free alloys for which no such strong carbide-forming element as hafnium was present (which limited the oversaturation of the ferritic matrixes of the three Hf-containing iron-based alloys. Consequently, the reject by the matrix of the carbon in excess did not induce a so great softening of these Hf-containing alloys as for the Hf-free ternary alloys. Contrarily, with the

increase in volume fraction of chromium carbides, the 1100°C-exposure led, for the Hf-containing alloys, to final hardness slightly higher than in the as-cast condition.

In an earlier work[17], the microstructure evolution of similar Hf-rich iron-based alloys at high temperature was already studied, but 100°C higher (1200°C, same duration). It was noticed that, in contrast with what it appeared here, the volume fraction of the hafnium carbides was not slightly decreased but significantly increased (about 2.5vol.% HfC more) while the chromium carbides volume fraction, globally, significantly decreased. This led to hardness values, after exposure at 1200°C, which were slightly lower than in the as-cast Hf-containing alloys. Here (1100°C), the more little difference in stability between the chromium carbides and the HfC ones, which is lower than the one at 1200°C, allowed precipitating new chromium carbides during the high temperature exposure. This led here to slightly increased hardness for the Hf-containing alloys and not to the slight hardness decrease observed after 46h of exposure at 1200°C.

Besides the microstructure changes at high temperature and their consequences on the hardness of the alloys, the exposures in the synthetic air at 1100°C allowed having a first look at their behaviour in high temperature oxidation. Globally the Hf-containing alloys correctly behaved in this field, a little better than their Hf-free homologues, as proven by the existence of a protective continuous $(Cr,Fe)_2O_3$ layer all around the samples. However, starts of local fast oxidation were noticed at the end of these 46 hours of exposure. Although the Hf-containing alloys studied here behaved better than the analogous Hf-rich chromium rich iron-based alloys earlier studied in oxidation at 1200°C[18] (high oxidation rates assessed by thermogravimetry, thicker multi-constituted oxides), they are themselves probably chemically not resistant enough at the temperature considered in the present work (1100°C). Here too this point needs to be improved.

What was wished with the formation of a HfC carbide network in these iron-based alloys was a significant improvement of their mechanical resistance at high temperature, property which is usually considered as very weak at so high temperature for iron-based alloys. The creep test realized here with one of the three HfC-containing alloys suggests that the expected effect of the hafnium carbides is really obtained. Indeed, even if the bending test was performed under a load inducing a not very high tensile stress, the deformation (primary stage of creep), which was initially fast, was thereafter considerably slowed down. The secondary stage of creep was effectively characterized by a particularly low steady state rate. Since this is this stage which governs the lifetime of the alloys in the mechanical point of view at high temperature, the strengthening effect of the interdendritic network of the script-

like HfC carbides mixed with matrix may allow long sustainability in case of improved chemical resistance of the alloys.

Conclusion

Thanks to the high refractoriness of their iron-chromium base and to their HfC carbides which present morphological and repartition characteristics favourable to high mechanical resistance at high temperature, such HfC-containing iron-based alloys are potentially very interesting. However, rather fast solidification obviously exposes these alloys to subsequent metallurgical instabilities which let think that they probably need to be stabilized by thermal treatment prior to use. The HfC carbides seemingly did not significantly evolve during long time at temperatures as high as 1100°C and one can think that the mechanical properties will remain constant during service. The great improvement expected for the high temperature mechanical properties of these alloys and revealed here by a preliminary bending test which showed a very interesting creep resistance at 1100°C, clearly confirms that the presence of HfC carbides in so {high temperature}-weak alloys, is potentially, in this field, considerably beneficial for this alloy family. Concerning their high temperature oxidation behaviour, these alloys appeared as being neither worse nor really better than their Hf-free ternary homologues elaborated in the same conditions. Improvements of their oxidation resistance may be achieved by various means such as increase in their bulk Cr content or deposition of protecting coating. The high temperature oxidation part of this work will be also interestingly deepened by the study of the effect of residual elements which may be also present in case of industrially produced alloys issued from the model alloys studied here.

Acknowledgement

The authors gratefully thank Thierry Schweitzer who carefully prepared the samples for the exposures to high temperature as well as Pascal Villeger who performed the XRD runs.

References

[1] E. F. Bradley: Superalloys: A Technical Guide, ASM International, Metals Park (1988).

[2] D. Young: High Temperature Oxidation Oxidation and Corrosion of Metals, Elsevier Corrosion Series, Amsterdam (2008).

[3] P. Kofstad: High Temperature Corrosion, Elsevier Applied Science, London (1988).

[4] M. J. Donachie, S. J. Donachie: Superalloys: A Technical Guide (2nd edition), ASM International, Materials Park (2002).

[5] P. Berthod: J. Alloy Compd. 481 (2009) 746.

[6] Y. G. Kim: J. Mater. Sci. 13 (1978) 759.

[7] E. Nold, G. Ondracek: Prakt. Metallogr. 23 (1986) 268.

[8] W. R. Witzke: Metal. Trans. A 7A (1976) 443.

[9] B. L. Chen, A. Luo, K. S. Shin, D. L. Jacobson: Refract. Metal. : State-of-the-Art, Proc. Symp. TMS Fall Meet. 65 (1989).

[10] A. Luo, J. J. Park, D. L. Jacobson, B. H. Tsao, M. L Ramalingam: Scripta Metall. Mater. 29 (1993) 729.

[11] A. Luo, J. J. Park, D. L. Jacobson, B. H. Tsao, M. L Ramalingam: Mat. Sci. Eng. A-Struct. 177 (1994) 89.

[12] J. J. Park, D. L. Jacobson: Tungsten Tungsten Alloys, Proc. 1st Int. Conf. 241 (1993).

[13] J. J. Park: Int. J. Refract. Met. H. 17 (1999) 331.

[14] H. P. Gao, R. H. Zee: J. Mater. Sci. Lett. 20 (2001) 885.

[15] P. T. B. Shaffer: Handbooks of High-Temperature materials N°1. Materials Index, Plenum Press, 1964.

[16] P. Berthod: Oxid. Met., 64 (2005) 235.

[17] E. Conrath, P. Berthod: Int. J. Mater. Res. (formerly: Z. Metallkd.), 105 (2014) 717.

[18] P. Berthod, E. Conrath: Oxid. Met., 82 (2014) 33.

Table 1. Chemical compositions of all the alloys determined by SEM/EDS measurements (+/- 1wt.%)

Alloys	Cr	Hf	C
Fe25	26.4 ±0.2	0	0.25
Fe50	28.4 ±1.2	0	0.50
Hfe25	25.8 ±0.5	4.8 ±1.8	0.25
Hfe50	25.9 ±1.1	4.0 ±0.6	0.50
HFE50	27.5 ±0.5	5.8 ±1.1	0.50

Table 2. Samples' masses before and after exposure at high temperature; resulting masses variations (all measurements done at room temperature)

Alloys (sample area/cm²)	Initial mass (mg)	Final mass (mg)	Mass variation per surface unit area (mg/cm²)
Fe25 (1.86)	752.4	773.2	11.1
Fe50 (1.25)	425.6	432.5	5.52
Hfe25 (1.45)	520.6	501.2	-13.4
Hfe50 (1.54)	626.2	628.9	1.75
HFE50 (1.45)	607.2	625.2	12.4

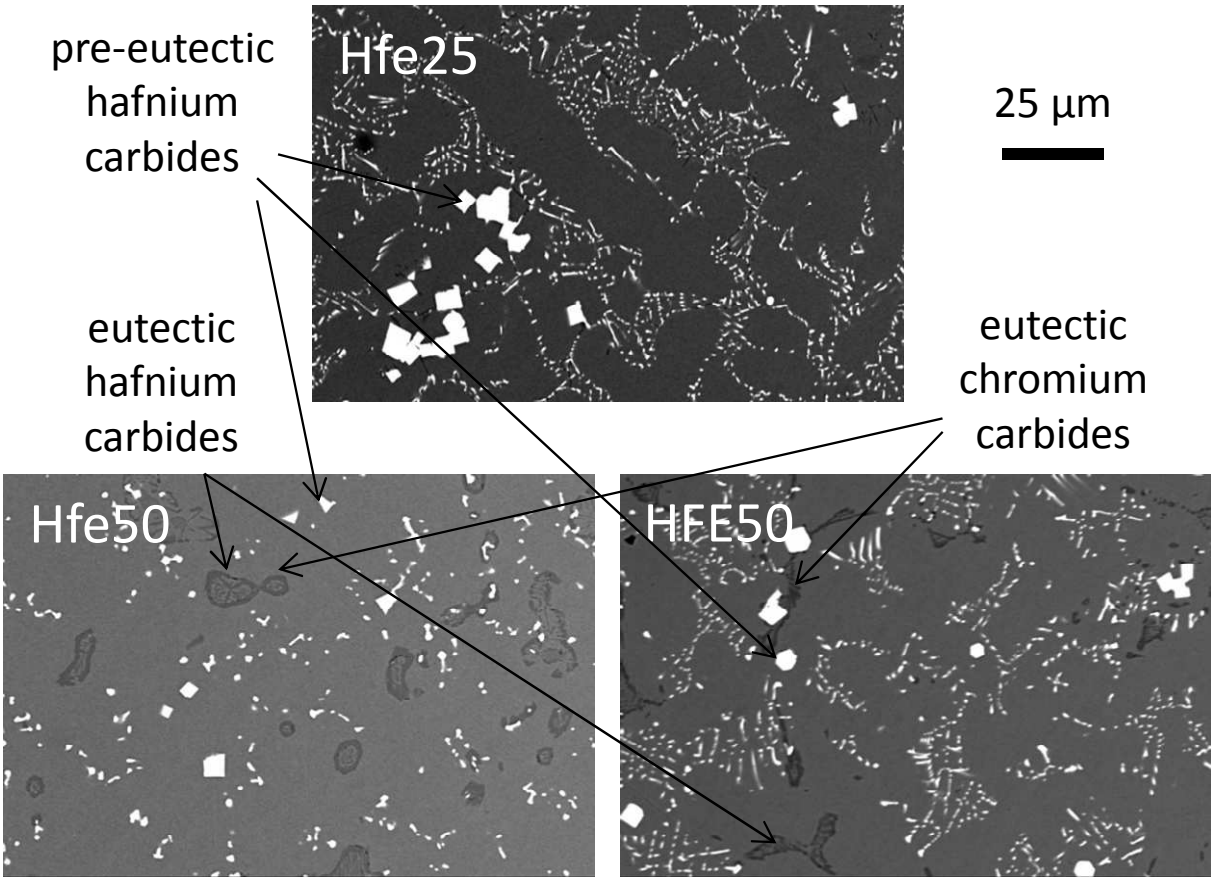

Fig. 1 As-cast microstructures of the HfC-containing alloys (top: Hfe25, bottom left: Hfe50, bottom right: HFE50); SEM/BSE micrographs

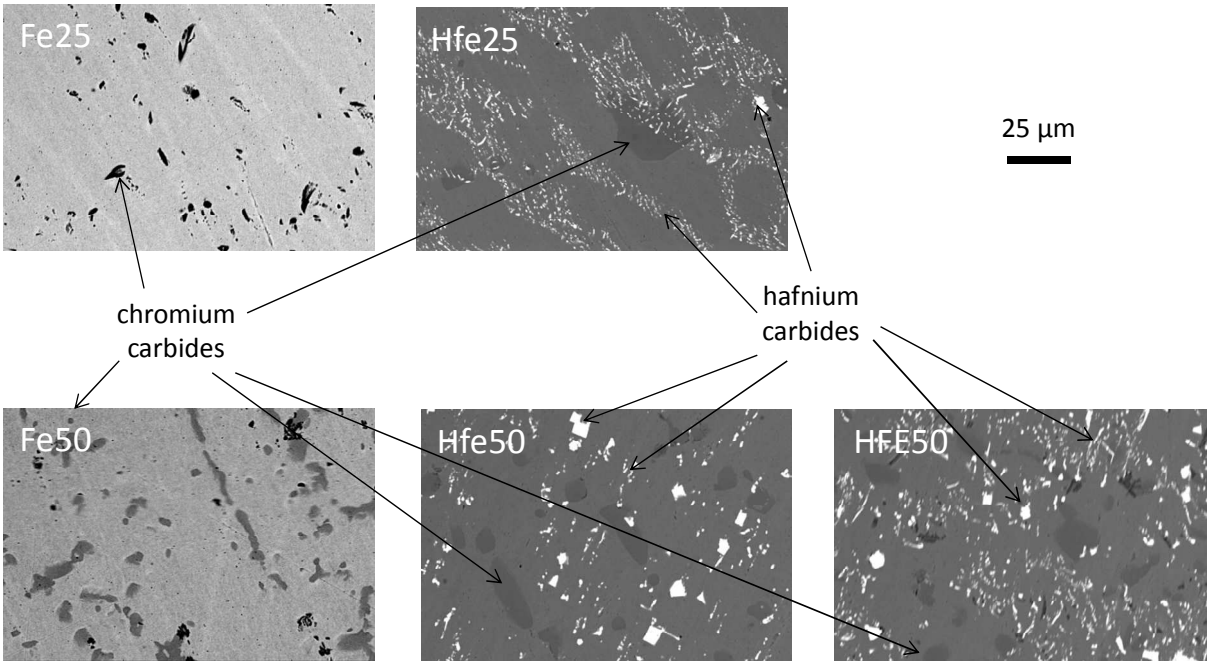

Fig. 2 {46h, 1100°C}-aged microstructures of the five alloys (SEM/BSE micrographs)

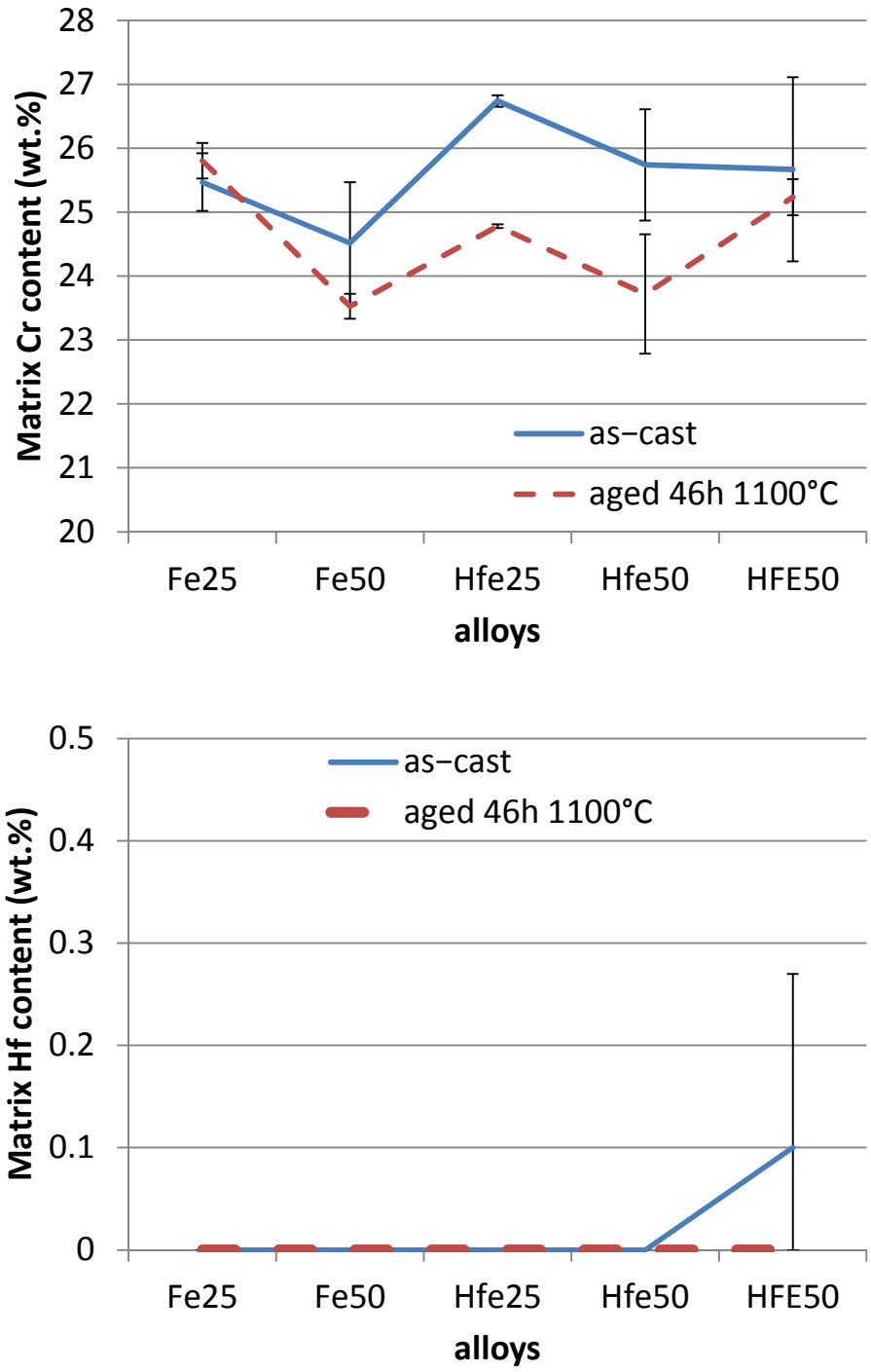

Fig. 3 Cr (top) and Hf (bottom) contents in the matrix of the five alloys in their as-cast states and in their aged states (EDS measurements, average and standard deviation values in each case)

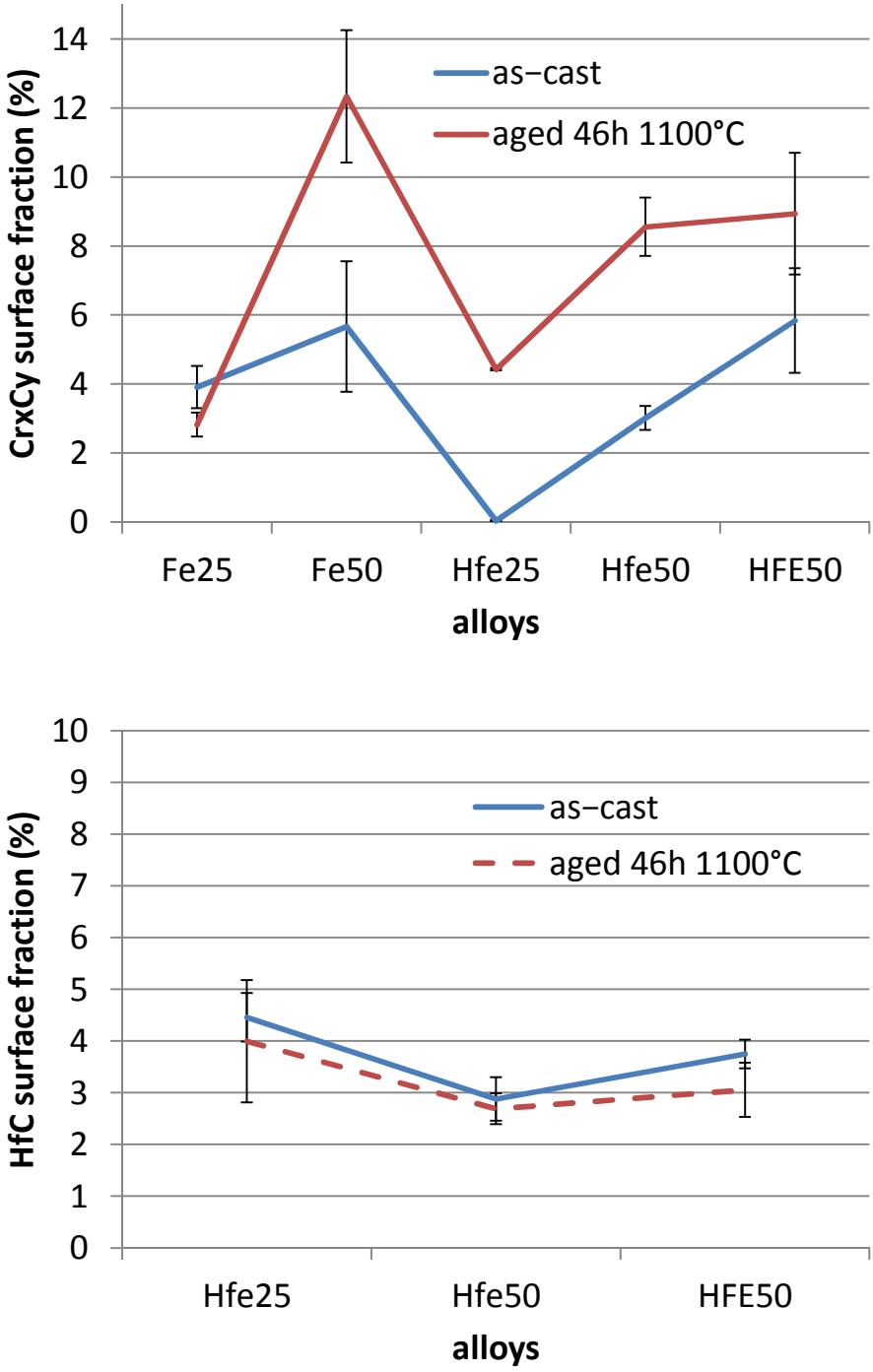

Fig. 4 Surface fractions of carbides in the five alloys in their as-cast states and in their aged states (top: chromium carbides, bottom: hafnium carbides)

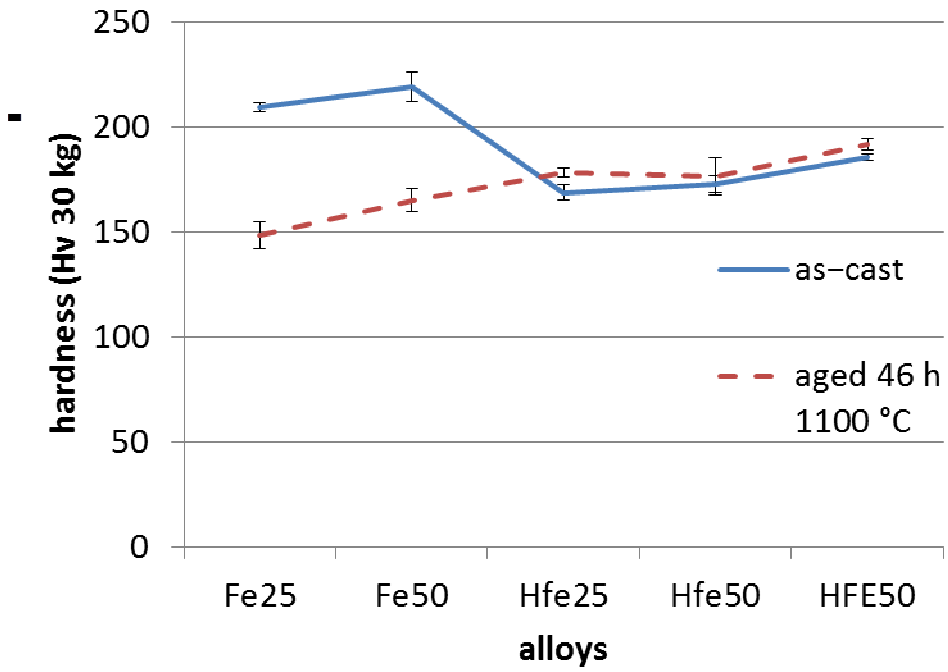

Fig. 5 Hardness of the five alloys in their as-cast states and in their aged states (Vickers method, 30kg load)

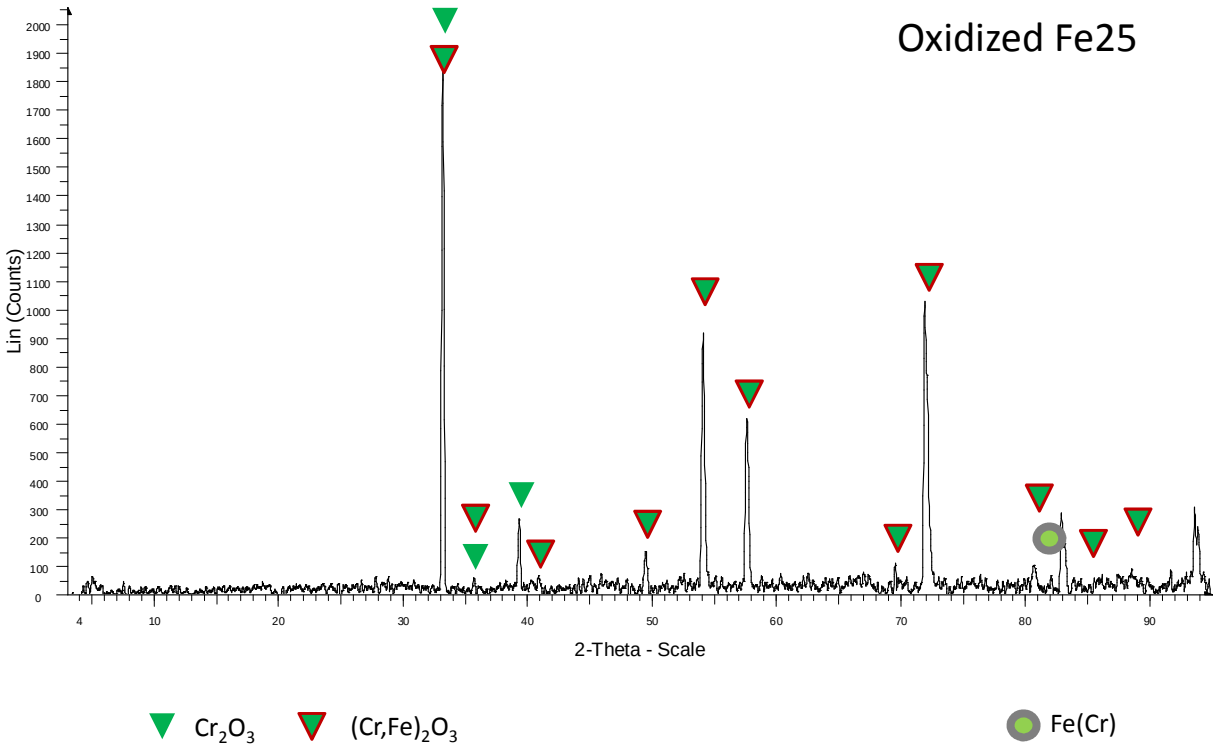

Fig. 6 Diffractogram obtained by XRD on the surface of the oxidized Hf-free Fe25 alloy

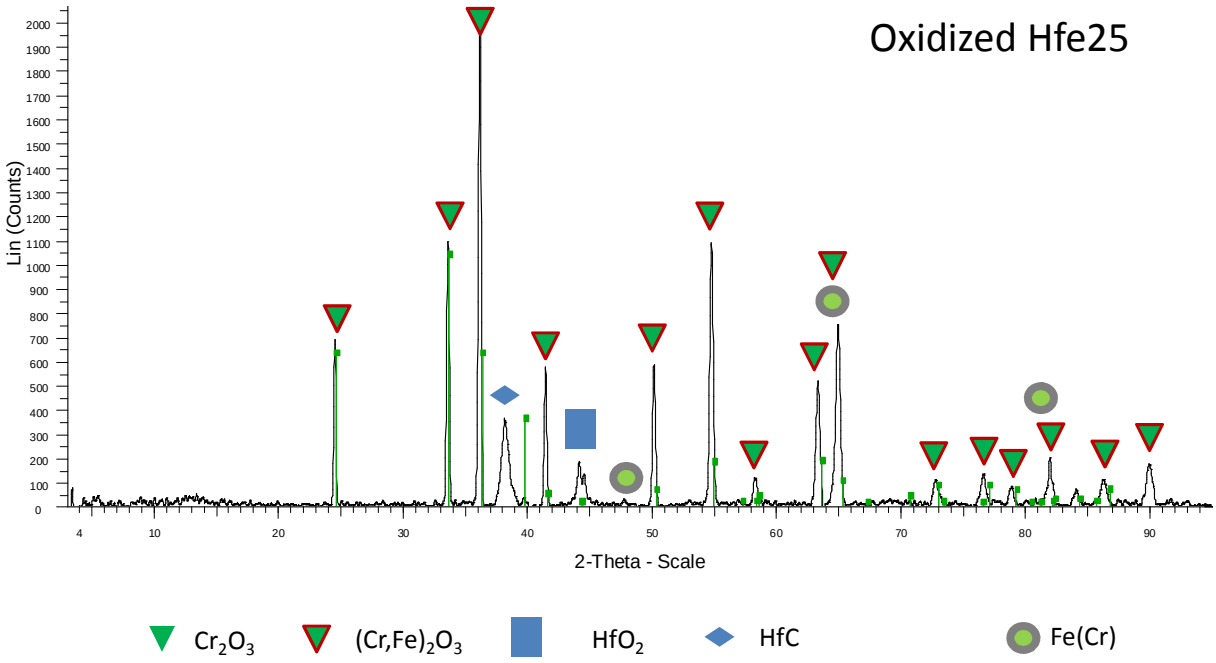

Fig. 7 Diffractogram obtained by XRD on the surface of the oxidized Hf-rich Hfe25 alloy

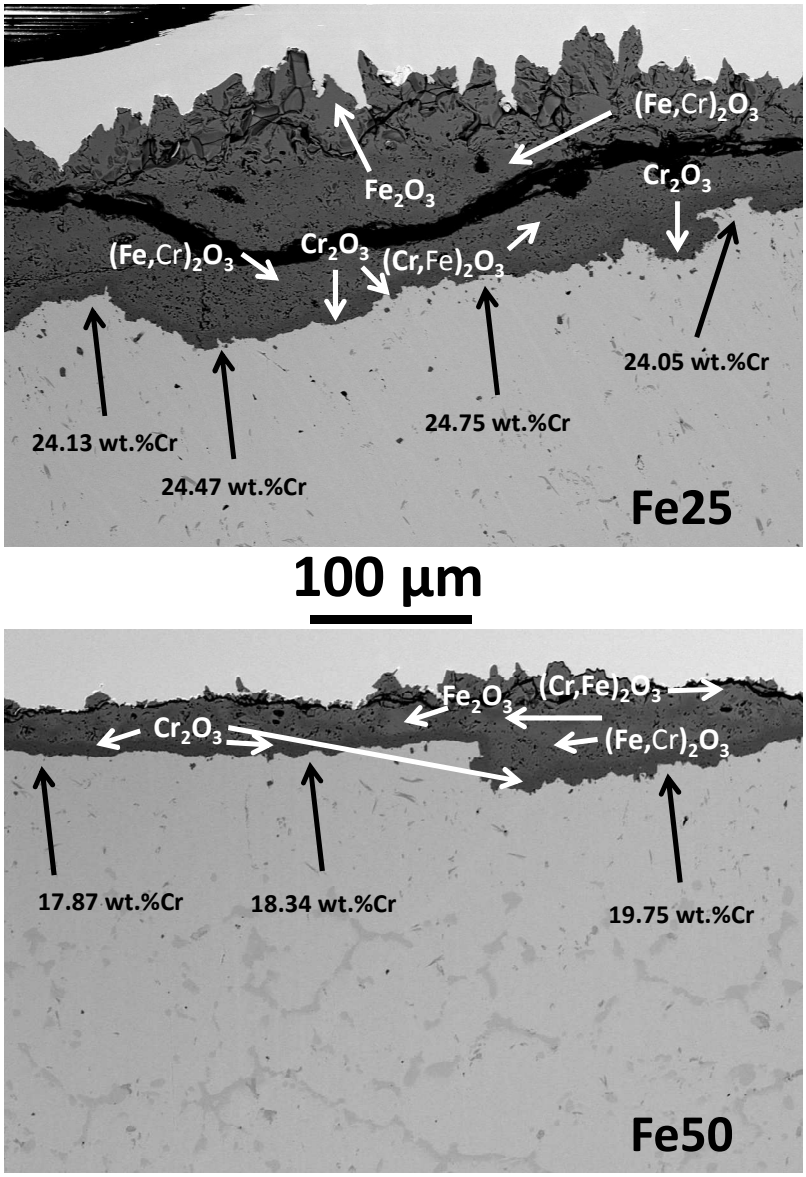

Fig. 8 Surface states of the two Hf-free alloys (top: Fe25, bottom; Fe50); identified oxides and sub-surface local chromium contents close to the oxide/alloy interface

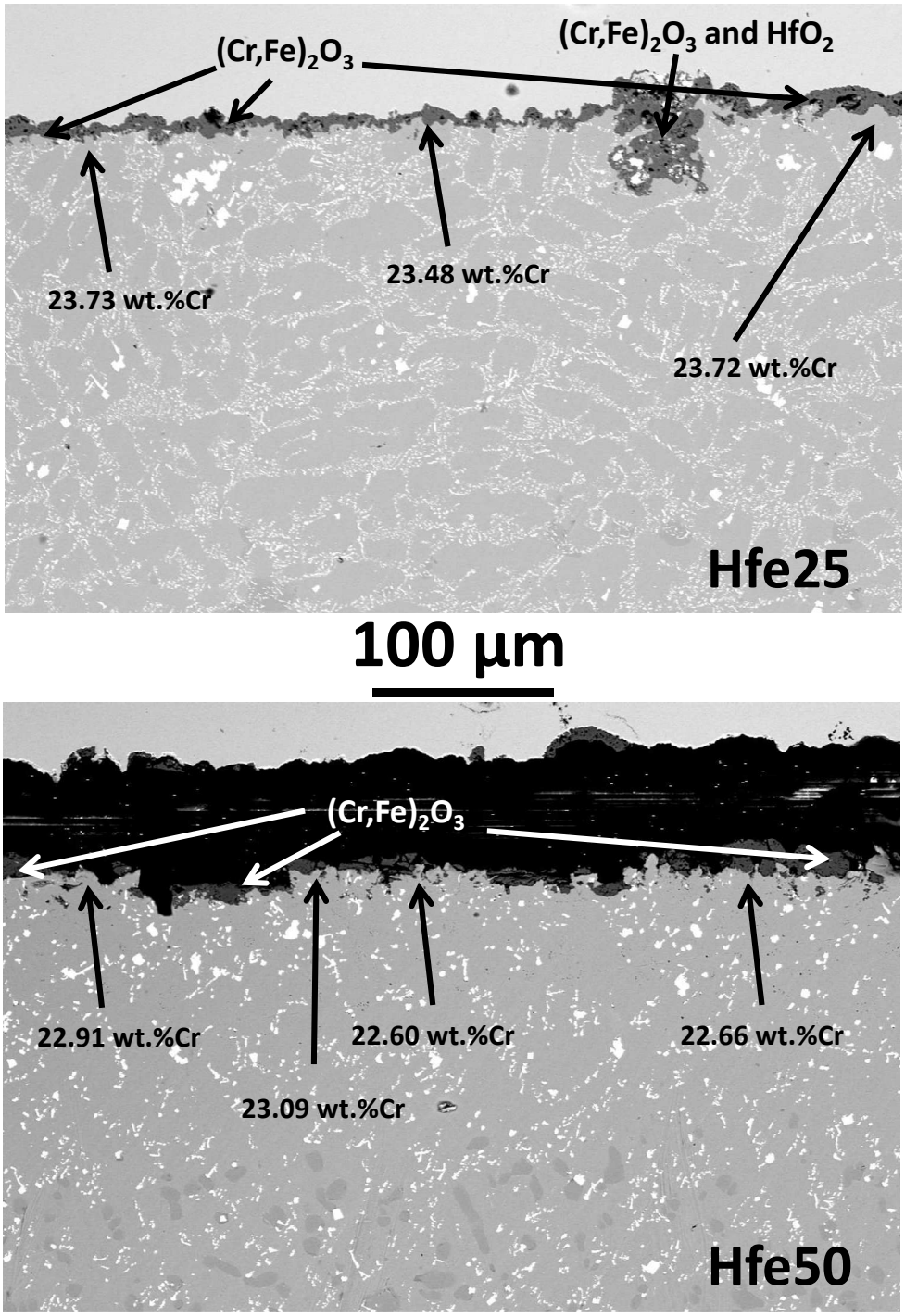

Fig. 9 Surface states of two of the three Hf-rich alloys (top: Hfe25, bottom left: Hfe50); identified oxides and sub-surface local chromium contents close to the oxide/alloy interface

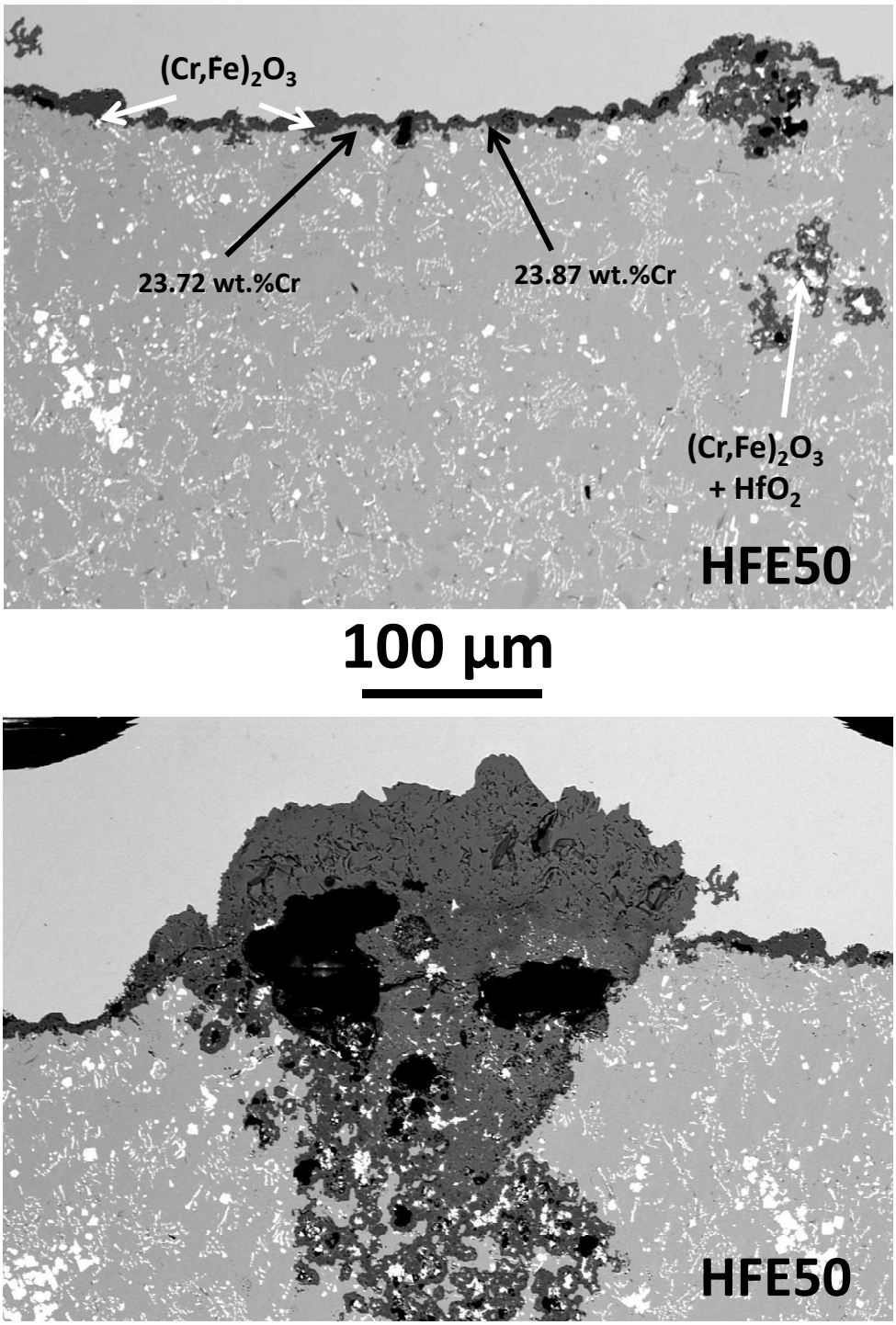

Fig. 10 Surface state of the oxidized HFE50 Hf-richest alloy (top: zone of still slow oxidation, bottom: zone of already fast oxidation)

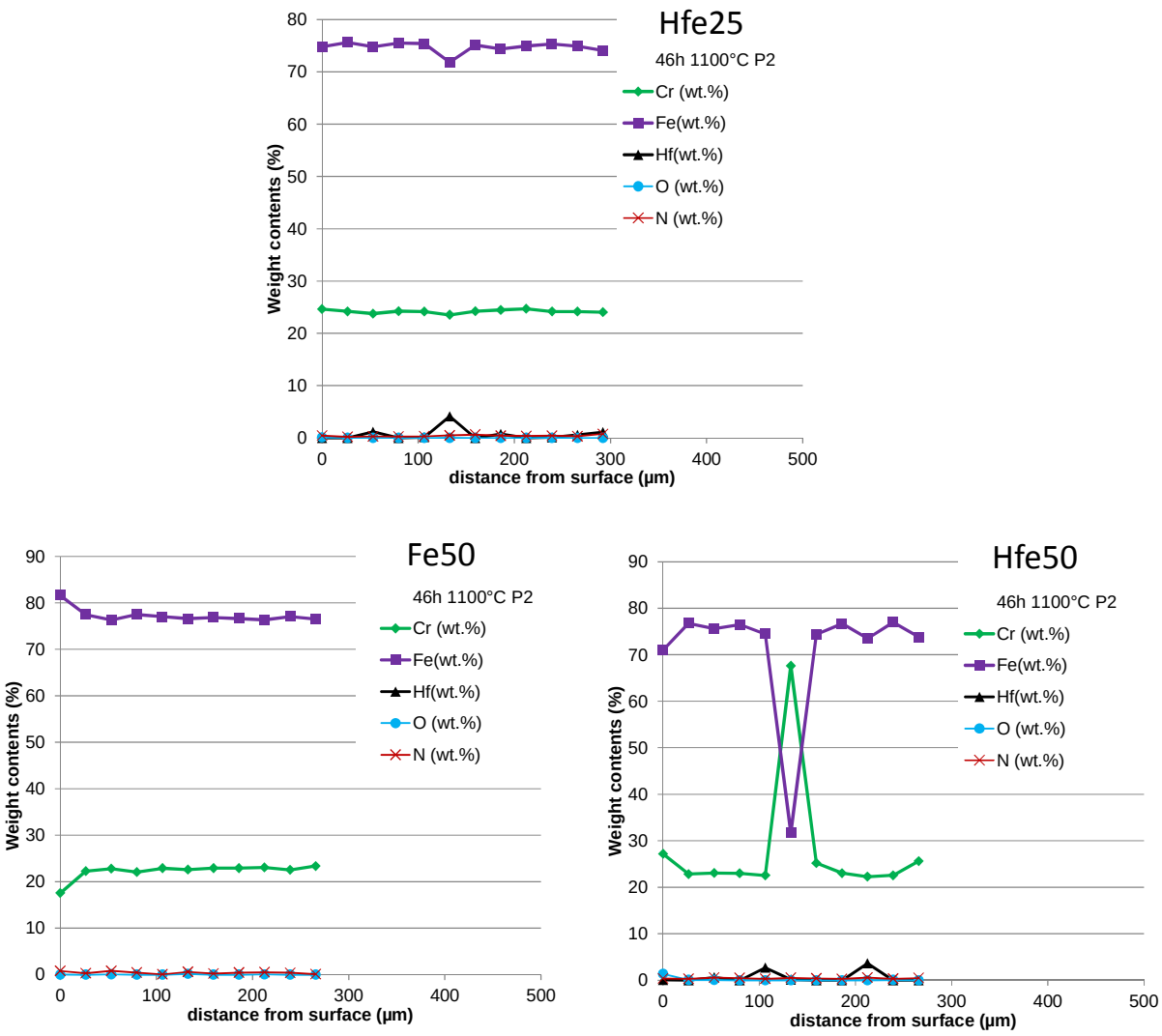

Fig. 11 Examples of concentration profiles through the sub-surface perpendicularly to the oxide/alloy interface (top: Hfe25, bottom left: Fe50, bottom right: Hfe50)

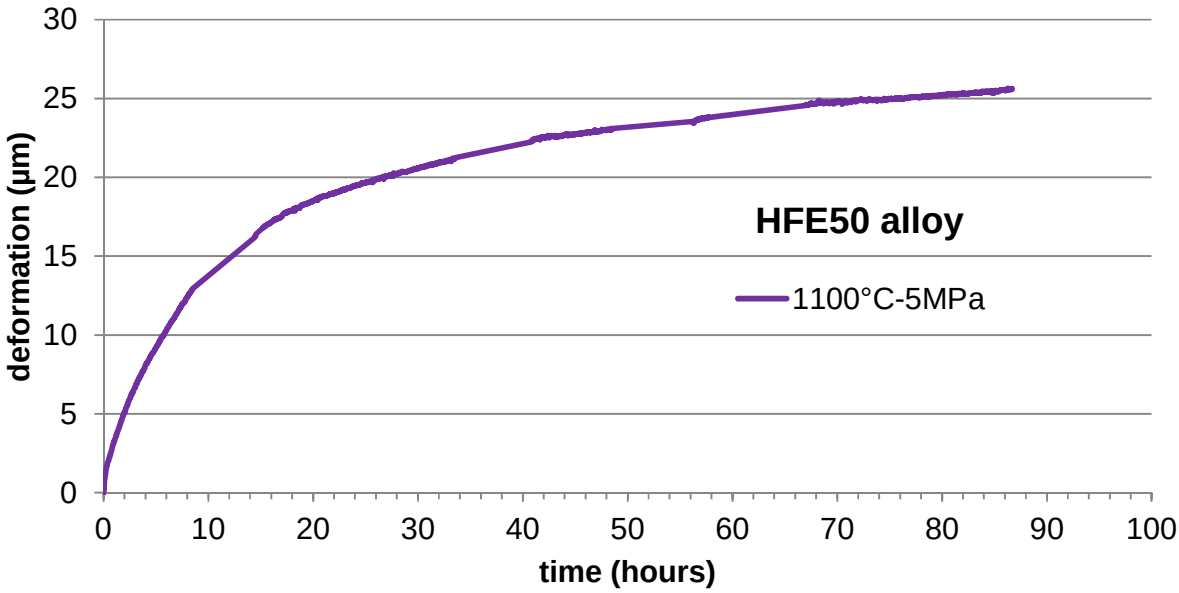

Fig. 12 Creep deformation of the HFE50 alloy during a {3 points}-bending test at 1100°C under a constant load inducing a tensile stress of 5 MPa in the middle of the bottom part of the parallelepiped sample